Dual interband cascade laser based trace-gas sensor for environmental monitoring

Gerard Wysocki,[1,*] Yury Bakhirkin,[1] Stephen So,[1] Frank K. Tittel,[1] Cory J. Hill,[2] Rui Q. Yang,[2] and Matthew P. Fraser[3]

[1]Department of Electrical and Computer Engineering, Rice University, 6100 Main Street, Houston, Texas 77251, USA
[2]Jet Propulsion Laboratory, California Institute of Technology, 4800 Oak Grove Drive, Pasadena, California 91109, USA
[3]Department of Civil and Environmental Engineering, Rice University, 6100 Main Street, Houston, Texas 77251, USA

*Corresponding author: gerardw@rice.edu

Received 18 July 2007; accepted 27 September 2007;
posted 3 October 2007 (Doc. ID 85453); published 19 November 2007

The development of an interband cascade laser (ICL) based spectroscopic trace-gas sensor for the simultaneous detection of two atmospheric trace gases is reported. The sensor performance was evaluated using two ICLs capable of targeting formaldehyde (H_2CO) and ethane (C_2H_6). Minimum detection limits of 3.5 ppbV for H_2CO and 150 pptV for C_2H_6 was demonstrated with a 1 s integration time. The sensor was deployed for field measurements of H_2CO, and laboratory quantification of both formaldehyde and ethane are reported. A cross comparison of the atmospheric concentration data for H_2CO with data collected by a collocated commercial H_2CO sensor employing Hantzsch reaction based fluorometric detection was performed. These results show excellent agreement between these two different approaches for trace-gas quantification. In addition, laboratory experiments for dual gas quantification show accurate, fast response with no crosstalk between the two gas channels. © 2007 Optical Society of America

OCIS codes: 280.3420, 300.6360, 300.6320, 280.1120.

1. Introduction

Elevated concentration levels of ground-level ozone are the most serious air quality issue facing many urban areas today. Ground-level ozone is formed by the photochemical reactions of volatile organic compounds (VOCs) and nitrogen oxides (NOx). Since ozone is not directly emitted from sources, but rather formed through atmospheric chemical reactions, air quality improvement plans must incorporate scientific understanding of how emissions, chemistry, and transport convert precursor VOCs and NOx into ozone. As a result, less progress has been made in attaining the health-based National Ambient Air Quality Standard (NAAQS) for ozone than for other pollutants regulated by the NAAQS that are directly emitted from sources (such as carbon monoxide or lead). In order to enable studies of this complex ozone chemistry, monitoring of several potential precursor molecules is required. Trace gas sensing methods that can provide *in situ*, fast (~1 s response time) and sensitive (at ppb and lower levels) detection of molecules of interest can greatly aide in understanding the atmospheric chemistry of ozone precursors. All these requirements can be successfully addressed by laser spectroscopic trace-gas detection, which proves to be one of the most sensitive gas sensing techniques and enables *in situ* real time measurements of trace gases for environmental [1,2], industrial [3,4], biomedical [5,6], and fundamental science applications [7].

The strongest fundamental absorption features of molecular species can be found in the midinfrared (mid-IR) spectral region (~3–20 μm). There are several mid-IR continuous wave (cw) laser sources that can be used for chemical sensing, e.g., semiconductor lasers, high power gas lasers (e.g., CO_2 and CO lasers), or nonlinear frequency conversion based mid-IR sources such as difference frequency generation sources or optical parametric oscillators. Due to their compact size and relatively simple operation requirements, semiconductor sources tend to be the most widely used in field instrumentation. For many

0003-6935/07/338202-09$15.00/0
© 2007 Optical Society of America

years, semiconductor diode lasers based on lead alloy semiconductors (e.g., PbSnTe) have been used as spectroscopic mid-IR light sources [1,8]. However, low output powers (~0.1–1 mW) and laser frequency instability caused by the thermal cycling strongly limit their reliability and range of applications. In the recent decade, rapidly developing new mid-IR semiconductor laser technologies such as interband cascade lasers (ICLs) and quantum cascade lasers (QCLs) have provided more reliable and viable laser sources for expanded applications of mid-IR laser spectroscopy. QCLs offer high power (up to 500 mW cw), room temperature operation, broad spectral coverage (3–170 μm), small size, and commercial availability. However, material systems that can provide reliable operation of QCLs at wavelengths shorter than 4 μm are still under development. This spectral region, which contains absorption bands associated with a fundamental vibrational mode of the C—H molecular group stretch in a number of molecules (especially hydrocarbons), is accessible using ICL technology. Availability of ICLs operating in cw near room temperatures (~260 K accessible with single-stage thermoelectric coolers) is still limited, but has been demonstrated in the Fabry–Perot version [9,10,11] and in the distributed feedback (DFB) version with stable single-mode operation [12]. At low temperatures (e.g., ~80 K), ICLs exhibited high cw powers (>100 mW) and extremely low threshold current density (e.g., ~5 A/cm^2 [11]) with low power consumption. The progress in this technology has been rapid, and room temperature cw operation is expected to be widely available with further development in the near future. In the meantime, however, systems based on ICL technology require cryogenic cooling of these laser sources.

Due to limited wavelength coverage of an individual laser source, laser spectroscopic trace-gas sensors are very often limited to a single molecular species that can be targeted with a particular laser. The capability for a single sensor to quantify multiple gas species is of great importance to atmospheric chemistry [1,13,14]. In order to address this issue, in this work we report on the development of a dual semiconductor laser based spectroscopic trace-gas sensor, which is capable of employing any type of mid-IR semiconductor laser that requires an operating temperature anywhere between LN_2 temperature (77 K) and room temperature (RT). The sensor platform was evaluated using two ICLs operating at cryogenic temperatures and targeting molecular absorption lines of formaldehyde (H_2CO) and ethane (C_2H_6), at 3.56 μm and 3.33 μm, respectively. Field tests of the sensor were performed in August and September 2006 during the Texas Air Quality Study II measurement campaign (TexAQS II).

2. Experimental Details

A. Sensor Architecture

The sensor architecture is schematically shown in Fig. 1. Two semiconductor lasers are mounted in a LN_2 dewar (Cryo Industries; custom LN_2 dewar). The dewar is equipped with two separately temperature-controlled cold fingers, which allows the use of two lasers with different operating temperatures. The two laser beams are collimated using two ZnSe aspheric lenses (diameter d = 25 mm and focal length of f = 12.5 mm). For beam tracing purposes a dichroic mirror (ISP Optics, model BSP-DI-25-3) was used to coalign a He–Ne laser beam (λ = 630 nm) with one of the mid-IR lasers. The collimated mid-IR beams, which are ~20 mm in diameter, are overlapped using a pellicle beam splitter (Thorlabs, model BP145B4, splitting ratio 45/55%). The beam splitter provides two dual-color laser beams in two separated optical channels that are used as a sample and reference beam for further concentration measurements. The thickness of the pellicle membrane is negligible, allowing suppression of beam ghosts, formation of small free spectral range (FSR) etalon fringes (only long FSR etalons can occur, which are much broader then the laser scan range), and minimal beam displacement (particularly important for a two laser system where both beams in the two channels must be well overlapped). The size of the sample beam is reduced to ~2.5 mm using an optical telescope consisting of two ZnSe lenses: (1) d = 25 mm, f = 25 mm, and (2) d = 6 mm, f = 3 mm. The sample beam was subsequently coupled to a 100 m astigmatic Herriott multipass cell using an additional BaF_2 lens (d = 25 mm, f = 500 mm). The beam exiting the multipass cell is focused onto a thermoelectrically cooled mercury-cadmium-telluride (MCT) photodetector using an off-axis parabolic mirror (d = 25 mm, f = 75 mm). The reference beam is used for laser wavelength monitoring and is directed through two reference gas cells containing high concentration samples of target gases. The intensity of the reference beam is monitored using a second thermoelectrically cooled MCT detector. The output signal from each detector (sample and reference) is amplified by a dedicated transimpedance preamplifier and measured by two lock-in amplifiers (see next section for further details). The in-phase components of the measured signals are acquired and then analyzed by a laptop computer equipped with a data acquisition card (National Instruments, model NI-DAQ 6062E). The system is equipped with an automatic LN_2 refilling system, which enables ~72 hours of autonomous sensor operation. The overall system is controlled by self-developed LabView based software, which provides real time data acquisition and analysis, system control (including gas handling systems and LN_2 monitoring) and periodic self-calibration. When an Internet connection is available at the measurement site, the sensor can be operated remotely.

B. Trace-Gas Concentration Measurements

Wavelength modulation spectroscopy (WMS) is used as a primary trace-gas detection method. This allows dual laser trace-gas measurements to be performed simultaneously at two different wavelength modulation (WM) frequencies [15]. More than two channels

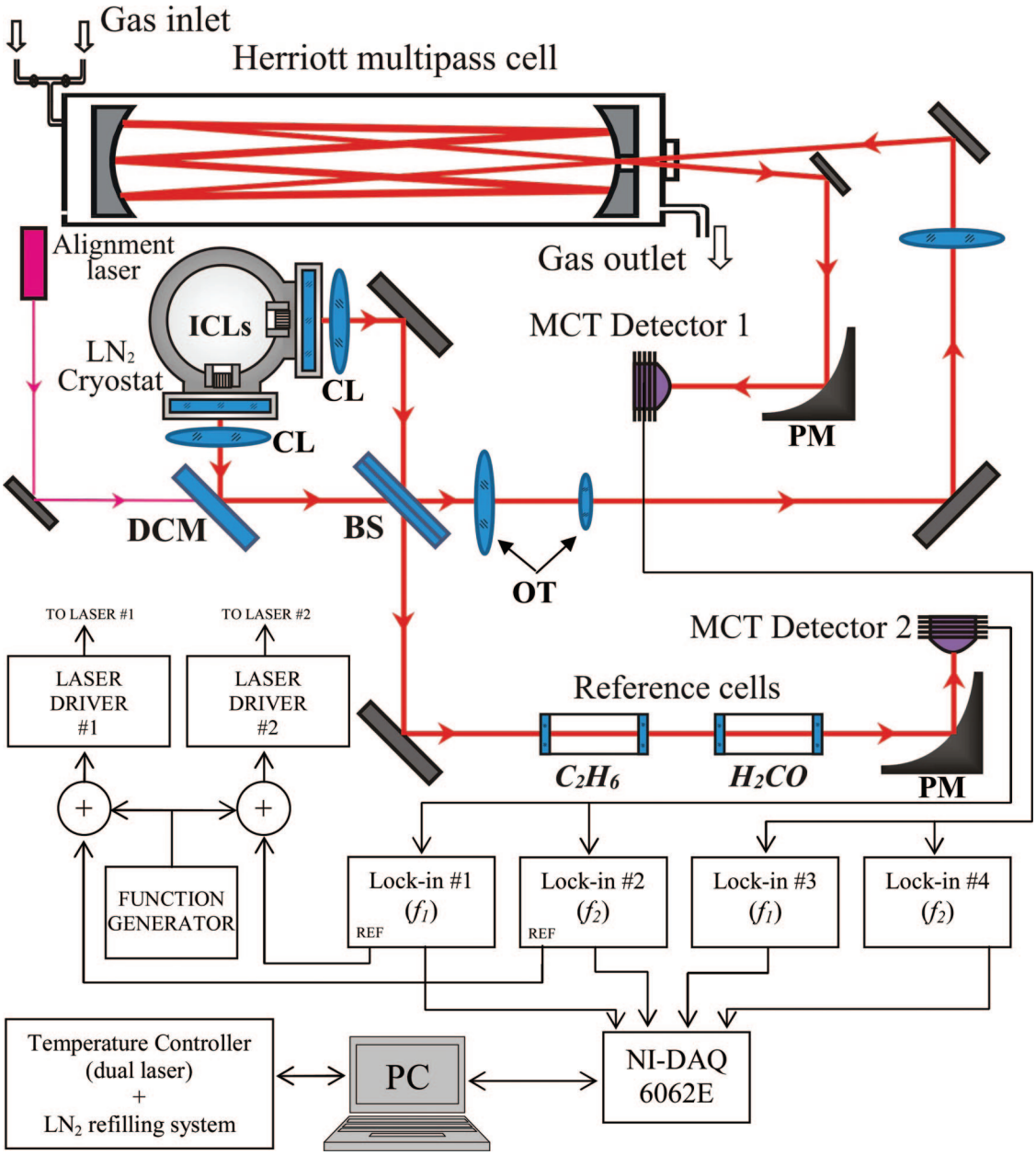

Fig. 1. (Color online) Schematic configuration of a dual ICL based trace gas sensor: ICL, interband cascade laser chip; DCM, dichroic mirror; BS, pellicle beam splitter; MCT, mercury-cadmium-telluride photodetector; CL, collimating lens; PM, off-axis parabolic mirror; OT, optical telescope, NI-DAQ, National Instruments data acquisition card.

can be introduced on one sensor platform without the need of increasing the number of photodetectors (costly in the mid-IR spectral region), and without the need for individual laser beam paths for each channel [1,13,14]. The software also allows configuration of the sensor for direct absorption measurements (with no sinusoidal WM), but in this mode only one laser at a time can be operated (dual laser operation can only be performed by alternating the laser duty cycles).

Each laser is supplied with a slow (10 Hz) sawtooth current waveform to perform a wavelength scan that covers the spectral region of interest (typically 0.5–1 cm^{-1}). In addition to a slow current ramp, the WM is performed using a high frequency sinusoidal current waveform at frequencies $f_1 = \sim 19$ kHz and $f_2 = \sim 24$ kHz added to the current waveforms of each respective laser. By using separate phase sensitive detection of the second harmonic at both modulation frequencies, the in-phase components of the $2f$ absorption signals originating from each laser can be measured using a single detector [15]. For the applied modulation parameters the data acquisition electronics allowed the collection of 5000 spectral points within each wavelength scan. The acquired spectral scans were averaged and then processed to calculate the concentration.

$2f$ WMS measures the second derivative of the measured absorption line shape, thus increasing

the immunity to slow baseline drifts and $1/f$ noise. This significantly improves instrument sensitivity in comparison to direct absorption spectroscopic measurements (typically by one order of magnitude). However, for concentration measurements, analytical or numerical simulation of $2f$ reference spectra requires a significantly more complex data analysis that takes into account such parameters as absorption line shape, optical power, laser wavelength modulation depth, calibration of the wavelength scan, residual modulation of the laser power, and detector response. Although precise modeling of the $2f$ spectra is theoretically feasible, in practice the $2f$ WMS based trace-gas sensors are usually calibrated using reference calibration gas mixtures [2,3]. In this work, the concentration is calculated by the correlation of a measured $2f$ spectrum with a reference spectrum, which is acquired for a known calibrated gas standard and stored in computer memory [2]. An important advantage of this technique is its capability to perform high precision gas concentration measurements (accuracy of the absolute instrument calibration is primarily related to the precision of the applied certified gas standard) without the need to determine any of the previously mentioned parameters, which are required for $2f$ spectra simulation. The fitting procedure uses a least-squares linear fit that employs a singular value decomposition (SVD) algorithm and is performed in real time (time between the consecutive concentration data points is determined by the number of spectral scans averaged).

Even small instabilities of the laser temperature can cause a spectral shift of the wavelength scan, which can lead to significant errors in the averaged data [16]. The temperature controller (LakeShore, model 340) and silicon diode temperature sensors provide a control stability of ~25 mK. Thermal fluctuations are usually slow and can be corrected using additional control loops employing fast laser wavelength tuning by means of the laser driving current. This technique can be used in a line-locked system that performs measurements at a single wavelength [3] as well as in a system performing laser frequency scanning of a spectroscopic feature of interest [5]. In a spectroscopic sensor that uses wavelength scanning, spectral channel shifting can be performed in software [16]. Such a method was applied in our system to eliminate laser frequency drifts caused by temperature fluctuations and other instabilities. The wavelength shift is determined using the $2f$ spectrum acquired in the reference channel and then applied to the data collected in the sample channel. In our system, two reference cells containing pure H_2CO and C_2H_6, respectively, were used. However, any molecule that has absorption features within the laser scan can be used for such a wavelength correction.

C. Laboratory Based Performance Tests

A laboratory evaluation test of the sensor was performed using two ICL lasers operating at 3.56 μm and 3.33 μm, respectively. Both lasers employed an embedded distributed feedback grating for single mode operation and could be operated in a cw mode up to temperatures of 150 K.

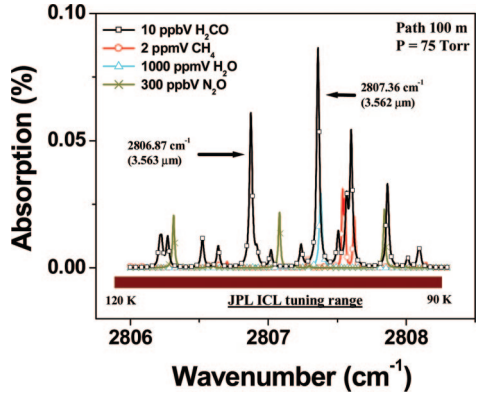

Fig. 2. (Color online) Simulated absorption spectrum of 10 ppbV H_2CO near 3.56 μm showing interferences including H_2O (1000 ppm), CH_4 (2 ppm) and N_2O (300 ppbV) at 75 Torr and with a 100 m effective optical path length.

The frequency of the 3.56 μm ICL tunes between 2805.7 and 2808.3 cm^{-1} by changing the temperature of the chip from 120 K to 90 K. This laser experienced a tendency for multimode generation, especially when operated at low temperatures and high driving currents. Single mode operation was obtained by careful selection of the cold finger temperature and the laser current. Within the overall laser tuning range, several strong absorption features of formaldehyde (H_2CO), one of the important molecules in ozone chemistry studies, can be used for sensitive concentration measurements (see Fig. 2). As depicted in the simulation spectrum of H_2CO absorption together with the absorption spectra of other molecules, which can cause the strongest spectral interference in this frequency range, the absorption line at 2806.87 cm^{-1} is the most suitable for sensitive formaldehyde detection. The strongest interference is caused by water (H_2O). Unlike the other interfering species [methane (CH_4), ~2 ppm in the atmosphere and nitrous oxide (N_2O) ~300 ppbV in the atmosphere], H_2O at normal atmospheric concentration levels (~1.6% calculated for 50% relative humidity at 25 °C) will significantly affect the measurements. The maximum acceptable H_2O concentration level, which provides minimal effects on the H_2CO measurements, is 0.1% (~3% relative humidity). There are several other H_2CO absorption lines in the 3.5 μm region, which are more optimal for sensitive measurements of H_2CO traces (e.g., 2734.2 cm^{-1}, 2749.2 cm^{-1}, 2754.9 cm^{-1}, 2759 cm^{-1}, 2831.64 cm^{-1} [8], and 2869.85 cm^{-1}); however, these spectral features cannot be targeted with the presently available ICL.

The frequency of the 3.33 μm ICL can be tuned thermally between 2991 and 2999.5 cm^{-1} by changing the temperature of the chip from 140 K to 90 K. This laser had a layer of antireflection coating (~5%) on its front facet and exhibited excellent single mode operation with a side mode suppression ratio of

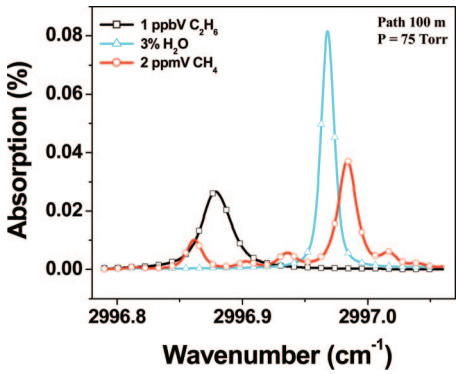

Fig. 3. (Color online) Simulated absorption spectrum of 1 ppbV C_2H_6 near 3.33 μm showing interferences including H_2O (3%), and CH_4 (2 ppm) at 75 Torr and with a 100 m effective optical path length.

SMSR > 20 dB. Sensitive concentration measurements of ethane (C_2H_6), which is an important molecule for environmental (C_2H_6 is tropospheric ozone precursor and tracer for anthropogenic emissions) [17,18] and medical (C_2H_6 is a biomarker for oxidative stress) [6] applications, can be performed in this spectral region. The optimum absorption line with minimal interference from other molecular species can be targeted at 2996.88 cm^{-1}. A simulation of the C_2H_6 absorption together with the absorption spectra of possible atmospheric spectral interferences (3% of H_2O and 2 ppm of CH_4) is shown in Fig. 3.

The sensitivity of the sensor was evaluated by measuring low concentration gas mixtures of C_2H_6 and H_2CO. The gas mixtures and zero gas (ultrahigh purity N_2) were alternated by the gas handling system into a multipass cell.

The C_2H_6 channel was tested using a certified mixture of 100 ppbV (±2%) of C_2H_6 in N_2 (Matheson Tri-Gas). All measurements were performed at a pressure of 75 Torr, which was optimized for the best selectivity and sensitivity. The scattering of the concentration measurements for both C_2H_6 mixture and the zero gas yielded a standard deviation of σ = ~150 ppt for 1 s integration time (see Fig. 4).

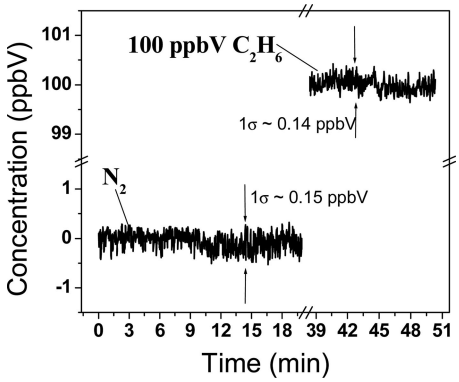

Fig. 4. Continuous monitoring of C_2H_6 performed over period of ~20 min with a zero gas and ~10 min with 100 ppbV mixture of C_2H_6 in N_2 flowing through the sensor system.

Stable concentration readings during a ~20 min period indicate good sensor stability. A bandwidth normalized minimum absorption detection limit of $\sim 3.6 \times 10^{-5}$ $Hz^{-1/2}$ (1 σ) was calculated for the C_2H_6 detection channel.

A similar test was performed for the H_2CO channel using a certified permeation based gas standard generator (Kin-Tek, model 491M). A standard deviation of the data points of σ = ~3.5 ppbV was observed for 1 s integration time, which yields a bandwidth normalized 1σ minimum absorption detection limit of $\sim 2.1 \times 10^{-4}$ $Hz^{-1/2}$. The factor of 6 lower performance of the H_2CO channel is mainly related to the lower spectral purity and instabilities of the 3.56 μm ICL available for this work.

The dual laser operation performance test was carried out using a custom mixture of ~79 ppbV of C_2H_6 and ~330 ppbV H_2CO in N_2 as a buffer gas. The linearity and the response time of the sensor were evaluated by diluting the custom gas mixture with pure N_2. The time series of the concentration measurements showing a five step dilution of the gas mixture (the steps correspond to a fraction of the initial concentration level of x = 1.0, 0.8, 0.6, 0.4, 0.2, and 0.0), and the subsequent reinjection of the initial mixture to the sample gas cell is presented in Fig. 5(a). The sensor response versus the dilution ratio

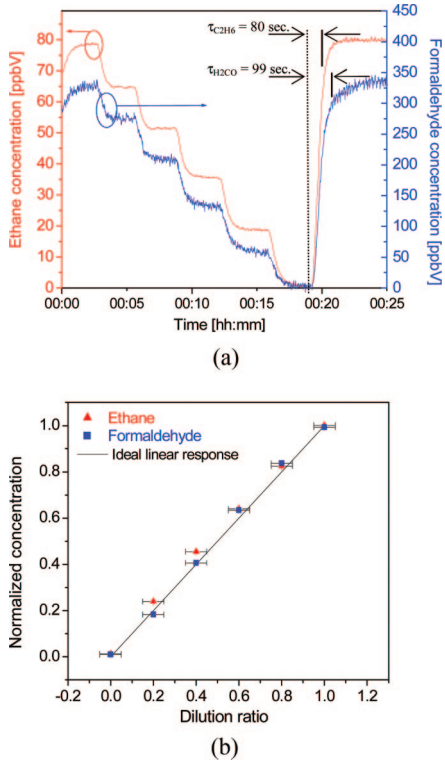

Fig. 5. (Color online) (a) Optical sensor response for two-channel operation targeting ethane (3.33 μm) and formaldehyde (3.56 μm). The initial gas mixture of ~330 ppbV H_2CO and ~79 ppbV C_2H_6 is gradually diluted by pure N_2. (b) Concentration measurements of ethane and formaldehyde normalized to their initial concentration level versus the dilution ratio (the error bars correspond to the precision of the dilution process).

shows a linear trend, which is depicted in Fig. 5(b) (the horizontal error bars represent the precision of the dilution). The measurements were performed using a gas flow of ~0.6 standard liter per minute. The overall volume of the sensor gas cell and the gas handling system recalculated for standard atmospheric pressure is ~0.5 liter. This corresponds to a time of ~50 s required for a complete gas exchange within the sensor volume. As shown in Fig. 5(a) a gas exchange time of 80 s was observed using the sensor response to step changes in the C_2H_6 concentration (time required to reach 90% of the signal level), which reasonably agrees with the expected system evacuation time. The time lag measured using the H_2CO time series corresponds to 99 s. This slower gas exchange is primarily determined by the chemical properties of H_2CO, which is a reactive species, soluble in water and known to adsorb easily to the walls of sensor system. To minimize the uncertainties in the H_2CO concentration measurements the system was operated with a constant gas flow.

The system was also tested for optical channel crosstalk in order to verify the quality of the measurement employing a single detector approach for phase-sensitive detection of two WMS signals at different modulation frequencies. In this test the same custom mixture (~79 ppbV of C_2H_6 and ~330 ppbV H_2CO in N_2) was diluted with a certified mixture of 100 ppbV of C_2H_6 in N_2. This allowed a decrease of the H_2CO concentration proportional to the dilution rate, while simultaneously increasing the initial C_2H_6 concentration based on the blend proportions. The time series of the concentration measurements showing a five step dilution process is depicted in Fig. 6. Similar dilution ratios to the previous test were used (x = 1.0, 0.8, 0.6, 0.4, 0.2, and 0.0). The dotted lines indicating the concentration values C_x for each level of ethane concentration are calculated using the initial value of 79.4 ppbV and the dilution factor x using $C_x = 79.4x + 100(1 - x)$. Excellent agreement of the expected value and the actual sensor reading can be clearly observed, which confirms the sensor linearity and demonstrates no crosstalk between the channels.

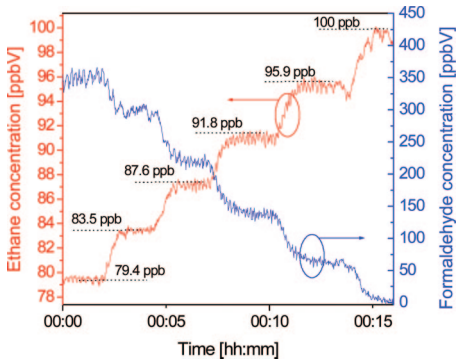

Fig. 6. (Color online) Two-channel optical sensor response to ethane and formaldehyde concentration in case of dilution of the initial gas mixture (same as in Fig. 5) with a mixture of 100 ppbV C_2H_6 in N_2.

D. Interband Cascade Laser Based Trace-Gas Sensor Field Test

In the Greater Houston area, where emissions from high concentration of petrochemical industrial sources combine with emissions from more traditional urban sources, the NAAQS for ozone is violated on roughly 45 days every year. Recently, emissions of volatile organic compounds (VOCs) from industrial sources have become the focus of air quality improvement plans in Houston, which are designed to reduce ambient ozone levels. Using aircraft sampling platforms and collecting whole air samples in evacuated stainless steel canisters that were then returned to a laboratory for analysis by gas chromatography, quantification of VOCs from industrial sources indicated significantly higher concentrations than expected [19,20]. Using this type of data and models of atmospheric dispersion, it has been estimated that the emissions for VOCs from industrial sources in Houston exceed previously estimated emissions by a factor of 5–10 [19,20]. As a result, the uncertainty in the emission inventory for VOCs is a major concern for air quality improvement plans in Houston.

Hence two of the most important trace gases to monitor for their ozone formation potential in Houston are ethylene (C_2H_4) and formaldehyde (H_2CO). Ethylene rapidly undergoes chemical oxidation, leading to the formation of both ground-level ozone and also formaldehyde. Rapid quantification of these two gases (formaldehyde and ethylene) simultaneously leads to an improved understanding of the chemistry of ozone formation. As demonstrated in the laboratory tests, the developed sensor in its present configuration is able to monitor H_2CO at ppb level, which is suitable for the atmospheric studies. Our initial goal was to configure the developed sensor to target both molecules (H_2CO and C_2H_4) simultaneously; however, at the time of our scheduled field test a suitable ICL targeting the ethylene was not available. The ICL based sensor described in this paper was deployed at the sampling site at the University of Houston main campus, which was one of the intensive monitoring sites in Houston during the TexAQS II campaign in August–September 2006. At this site a commercial formaldehyde sensor using Hantzsch reaction-based fluorometric detection was deployed by a research group from University of Houston lead by B. Rappenglueck, which provided an excellent opportunity for data intercomparison between an optical sensor and the traditional chemical technique.

As discussed in the previous section, the H_2CO measurements can be performed reliably when the humidity of the sample gas is kept at 3% or lower relative humidity level. During the summer months, the relative humidity in Houston is >90%, and the measurements could only be performed by using an air dryer at the system inlet. A very reliable and convenient gas dryer can be constructed using Nafion membrane tubing. It has been suggested [21] and verified in our experiments that concentration of H_2CO is affected when drawn through the Nafion

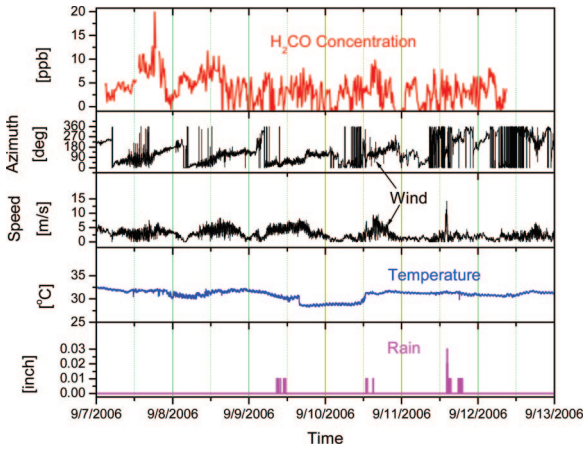

Fig. 7. (Color online) Continuous measurements of H_2CO collected during 5.5 day period with atmospheric data acquired at the sampling site.

dryer. Alternatively, efficient drying can also be performed using cooling traps. Under normal conditions, the freezing point of formaldehyde is at 155 K (a LN_2 cooling trap cannot be applied). A dry ice (solid CO_2) cooling trap with temperature of 194.6 K was therefore chosen for our H_2O trap in the system. The vapor pressure of H_2CO at this temperature is ~20 Torr, which corresponds to a concentration of ~2.6% at atmospheric pressure and is much higher than the expected atmospheric levels of H_2CO. Thus the measured H_2CO level should not be affected. This was confirmed during our experimental testing of the cooling trap in which the detected H_2CO levels and the sensor response time were identical with and without the cooling trap present at the sampling port. Similar behavior is also expected for C_2H_4, which is less reactive and water soluble than H_2CO, with saturated vapor pressure of 3000 Torr at dry ice temperatures. During the field test, a ~10 m sampling tube was used to deliver the atmospheric air to the sensor before the cooling trap. The tube was equipped with a resistive heater and kept at ~40 °C to avoid water condensation on the tube walls.

The laser dewar required periodic LN_2 refilling, which determined the actual measurement cycle. After each LN_2 refilling, a 20 min cool-down period was required to let the system stabilize thermally. The calibration and measurement sequence was initiated after the cool-down period. The pattern consisted of the following: (1) full calibration (including zero gas measurement followed by a reference gas measurement) performed after each LN_2 refilling; (2) sample measurement (10 min); and (3) zero gas calibration (occurred periodically after each 10 min sampling period until the next LN_2 refilling). The time between LN_2 refillings was primarily determined by the total power dissipation within the dewar, which includes the dissipation of the ICLs and the dissipation in the resistive heaters used for temperature control of the cold fingers. In the present configuration the refilling process occurred every ~6 hours. To assure uninterrupted operation of the system, a 50 liter LN_2 reservoir had to be refilled every ~72 hours. An example series of data collected continuously during a 5.5 day

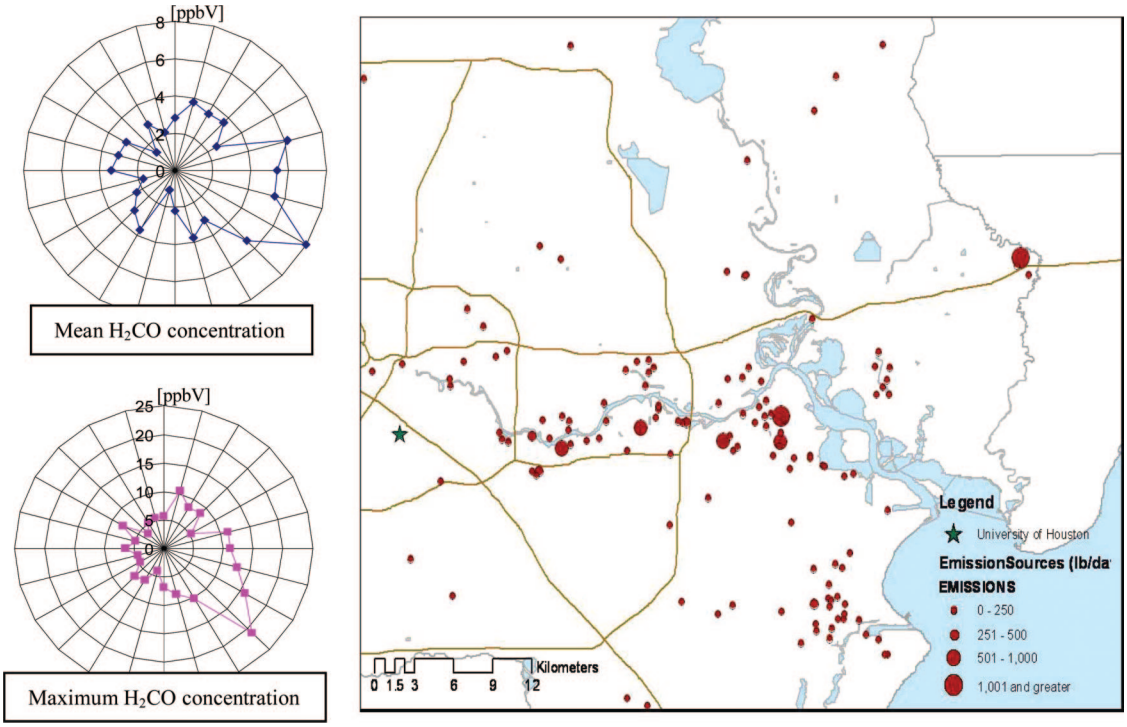

Fig. 8. (Color online) Mean level and maximum level of H_2CO concentration (ppbV) versus wind direction calculated using data from Fig. 7 (data averaged within 15° angles). The map on the right shows the sampling site (marked with "☆") and major VOC sources in the Greater Houston area, Harris County [22].

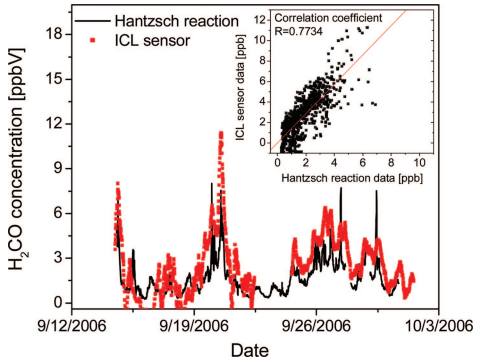

Fig. 9. (Color online) Measurements of H_2CO collected during ~2 week period with ICL-based trace gas sensor and with Hantzsch reaction based fluorometric detector. The inset shows a correlation of $R = 0.7734$ between data collected by the two different sensors located at the same sampling site.

period is shown in Fig. 7. As shown in the same figure, other atmospheric data such as wind direction and speed, temperature, and precipitation were also collected at the sampling site, which by appropriate correlation allows for more accurate atmospheric chemistry studies. The H_2CO measurements over the period 7–11 September 2006 were correlated with the wind direction, and the results are plotted in Fig. 8. Both the mean level and the maximum level of H_2CO concentration versus wind direction binned within 15° angle sections show clearly the industrial origin of H_2CO from the major VOC sources in Houston, Harris County (see the map in Fig. 8 for Ref. [22]).

During a ~2 week period between September 14th and 30th in 2006, the formaldehyde data collected by the ICL-based sensor could be correlated with the data collected by the Hantzsch reaction based fluorometric H_2CO sensor. Both sensors were deployed at the same sampling site; however, two different sampling ports were used to deliver the ambient air to each separate sensor. The results of this comparison are presented in the Fig. 9. The overall trend of both measurements is in very good agreement, and a correlation coefficient of $R = 0.7734$ was calculated (see inset in Fig. 9). There is a visible offset between the two measurements with an approximately 30% lower concentration levels being measured by Hantzsch reaction sensor in comparison to ICL sensor measurements. We suspect that this was due to significant differences in the respective sampling port construction with different H_2CO losses in sampling. At this time we do not have strong validation of this hypothesis, which will be investigated in more detail during future planned cross-comparison experiments.

3. Conclusions

For the monitoring of trace-gas levels of interest, the rapid response of an optical trace sensor has significant advantages over other techniques (e.g., chemical techniques) typically operating with a response time of 15 min to an hour. We have developed a dual ICL based trace-gas sensor and shown that spectroscopic quantification of two gases at separate wavelengths is feasible with a sub-ppb sensitivity and integration time of 1 s. Using two ICLs that targeted formaldehyde (H_2CO) and ethane (C_2H_6), the optical sensor showed a linear response for both gases with no crosstalk between gas channels. The sensor can accommodate any semiconductor lasers with operating temperatures of 77 K and higher (up to room temperature), which makes this instrument very flexible for a wide range of chemical sensing.

We plan to further evaluate the reported system with improved lasers for simultaneous quantification of H_2CO (a laser with better SMSR) and targeting the more reactive hydrocarbon C_2H_4 (instead of C_2H_6 as reported here). This will allow significantly more effective atmospheric chemistry studies, because the rapid oxidation of ethylene to formaldehyde is vital in the understanding of ground-level ozone chemistry. Ethane reacts slowly in the atmosphere and is less important than ethylene to ground-level ozone formation. With a dual optical sensor for H_2CO and C_2H_4, it is planned to perform further instrument intercomparison and atmospheric research studies at the University of Houston campus sampling site.

The authors wish to thank Bernhard Rappenglueck and Barry Lefer for their invaluable assistance and organization during the TexAQS II 2006 measurement campaign as well as for providing their measurement data for analysis. We also wish to thank our colleagues at Rice, Shagun Bhat and Rafal Lewicki, for logistical support. This work was performed with financial support from National Science Foundation Mid-Infrared Technologies for Health and the Environment (MIRTHE) Engineering Research Center and the Robert Welch Foundation. We acknowledge contributions from R. E. Muller and P. M. Echternach for e-beam writing of DFB gratings on lasers, B. Yang for laser device processing, Arch-com Technology, Inc., for facet coating, and C. M. Wong, J. Li, and Y. Qiu for a screening test of lasers. The development of DFB ICLs was carried out at Jet Propulsion Laboratory, California Institute of Technology, under contract with the National Aeronautics and Space Administration (NASA).

References

1. M. Loewenstein, H. Jost, J. Grose, J. Eilers, D. Lynch, S. Jensen, and J. Marmie, "Argus: a new instrument for the measurement of the stratospheric dynamical tracers, N_2O and CH_4," Spectrochim. Acta Part A **58,** 2329–2345 (2002).
2. A. Fried, J. R. Drummond, B. Henry, and J. Fox, "Versatile integrated tunable diode laser system for high precision: application for ambient measurements of OCS," Appl. Opt. **30,** 1916–1932 (1991).
3. W. H. Weber, J. T. Remillard, R. E. Chase, J. F. Richert, F. Capasso, C. Gmachl, A. L. Hutchinson, D. L. Sivco, J. N. Baillargeon, and A. Y. Cho, "Using a wavelength-modulated quantum cascade laser to measure NO Concentrations in the parts-per-billion range for vehicle emissions certification," Appl. Spectrosc. **56,** 706–714 (2002).
4. G. Wysocki, A. A. Kosterev, and F. K. Tittel, "Spectroscopic trace-gas sensor with rapidly scanned wavelengths of a pulsed quantum cascade laser for *in situ* NO monitoring of industrial exhaust systems," Appl. Phys. B **80,** 617–625 (2005).

5. A. A. Kosterev, F. K. Tittel, W. Durante, M. Allen, R. Koehler, C. Gmachl, F. Capasso, D. L. Sivco, and A. Y. Cho, "Detection of biogenic CO production above vascular cell cultures using a near-room-temperature QC-DFB laser," Appl. Phys. B **74,** 95–99 (2002).
6. D. Halmer, S. Thelen, P. Hering, and M. Muertz, "Online monitoring of ethane traces in exhaled breath with a difference frequency generation spectrometer," Appl. Phys. B **85,** 437–443 (2006).
7. S. C. Herndon, D. D. Nelson, Jr., Y. Li, and M.S. Zahniser, "Determination of line strengths for selected transitions in the v_2 band relative to the v_1 and v_5 bands of H_2CO," J. Quant. Spectrosc. Radiat. Transfer **90,** 207–216 (2005).
8. A. Fried, B. Henry, B. Wert, S. Sewell, and J. R. Drummond, "Laboratory, ground-based, and airborne tunable diode laser systems: performance characteristics and applications in atmospheric studies," Appl. Phys. B **67,** 317–330 (1998).
9. K. Mansour, Y. Qiu, C. J. Hill, A. Soibel, and R. Q. Yang, "Mid-infrared interband cascade lasers at thermoelectric cooler temperatures," Electron. Lett. **42,** 1034 (2006).
10. W. W. Bewley, C. L. Canedy, M. Kim, C. S. Kim, J. A. Nolde, J. R. Lindle, I. Vurgaftman, and J. R. Meyer, "Interband cascade laser operating to 269 K at $\lambda = 4.05$ μm," Electron. Lett. **43,** 39–40 (2007).
11. C. L. Canedy, W. W. Bewley, M. Kim, C. S. Kim, J. A. Nolde, D. C. Larrabee, J. R. Lindle, I. Vurgaftman, and J. R. Meyer, "High-temperature interband cascade lasers emitting at lambda = 3.6–4.3 μm," Appl. Phys. Lett. **90,** 181120 (2007).
12. R. Q. Yang, C. J. Hill, K. Mansour, Y. Qiu, A. Soibel, R. Muller, and P. Echternach, "Distributed feedback mid-infrared interband cascade lasers at thermoelectric cooler temperatures," IEEE J. Sel. Top. Quantum Electron. (to be published).
13. Y. Q. Li, K. L. Demerjian, M. S. Zahniser, D. D. Nelson, J. B. McManus, and S. C. Herndon, "Measurement of formaldehyde, nitrogen dioxide, and sulfur dioxide at Whiteface Mountain using a dual tunable diode laser system," J. Geophys. Res. **109,** D16S08 (2004).
14. R. Jimenez, S. Herndon, J. H. Shorter, D. D. Nelson, J. B. McManus, and M. S. Zahniser, "Atmospheric trace gas measurements using a dual quantum-cascade laser mid-infrared absorption spectrometer," Proc. SPIE **5738,** 318–331 (2005).
15. D. B. Oh, M. E. Paige, and D. S. Bomse, "Frequency modulation multiplexing for simultaneous detection of multiple gases by use of wavelength modulation spectroscopy with diode lasers," Appl. Opt. **37,** 2499–2501 (1998).
16. P. Werle, "Signal processing strategies for tunable diode laser spectroscopy," Proc. SPIE **2112,** 19–30 (1994).
17. C. P. Rinsland, N. B. Jones, B. J. Connor, S. W. Wood, A. Goldman, T. M. Stephen, F. J. Murcray, L. S. Chiou, R. Zander, and E. Mahieu, "Multiyear infrared solar spectroscopic measurements of HCN, CO, C_2H_6, and C_2H_2 tropospheric columns above Lauder, New Zealand (45°S latitude)," J. Geophys. Res. **107,** 4185.1.1–4185.1.12 (2002).
18. Y. Zhao, K. Strong, Y. Kondo, M. Koike, Y. Matsumi, H. Irie, C. P. Rinsland, N. B. Jones, K. Suzuki, H. Nakajima, H. Nakane, and I. Murata, "Spectroscopic measurements of tropospheric CO, C_2H_6, C_2H_2, and HCN in northern Japan," J. Geophys. Res. **107,** 4343.2.1–4343.2.13 (2002).
19. L. I. Kleinman, P. H. Daum, D. Imre, Y. N. Lee, J. L. Nunnermacker, S. R. Springston, J. Weinstein-Lloyd, and J. Rudolph, "Ozone production rates and hydrocarbon reactivity in five urban areas: a cause for high ozone concentrations in Houston," Geophys. Res. Lett. **29,** 1467.105.1–1467.105.4 (2002).
20. T. B. Ryerson, M. Trainer, W. M. Angevine, C. A. Brock, R. W. Dissly, F. C. Fehsenfeld, G. J. Frost, P. D. Goldan, J. S. Holloway, G. Hubler, R. O. Jakoubek, W. C. Kuster, J. A. Neuman, D. K. Nicks, D. D. Parrish, J. M. Roberts, and D. T. Sueper "Effect of petrochemical industrial emissions of reactive alkenes and NOx on tropospheric ozone formation in Houston, Texas," J. Geophys. Res. **108,** 4249.8.1–4249.8.24 (2003).
21. http://www.permapure.com/TechNotes/Formaldehyde.htm.
22. Texas Commission on Environmental Quality (2006) Point Source Emission Inventory Database, provided by TCEQ Technical Analysis Division, Austin, TX.